



Characterization of an electro dialytic cell: automation and process control

José A. Ibáñez Mengual, Ramón Valerdi Pérez*, Felipe Carbonell Bejerano

Departamento de Física Campus de Espinardo, Universidad de Murcia, 30071 Murcia, España, Tel. +34 868883942; Fax: +34 868884148; email: jaibanez@um.es (J.A. Ibáñez Mengual), valerdi@um.es (R. Valerdi Pérez), carbonellbejerano.antonio@um.es (F. Carbonell Bejerano)

Received 15 July 2014; Accepted 19 November 2014

ABSTRACT

Electrodialysis uses ion-exchange membranes to reduce the ionic content of electrolyte solutions by means of an electric field. The flow of ions removed through this process is limited by the effect of concentration polarization on the interfaces between the membranes and adjacent solutions. This work provides a methodology applicable to a single electro dialytic cell consisting of an anion membrane, a spacer of demineralizate, a cation membrane and a spacer of concentrate, the whole system located between two metal plates containing two electrodes (anode and cathode). All the items are commercially available and belong to a pilot electro dialysis reversal (EDR) plant *Aquamite I* of *Ionics*. The experimental procedure is based on the establishment of successive potential electric differences between the electrodes in order to determine current intensities at different work pressures. Thus, the current–voltage curves are drawn from where it follows the intensities of limiting current intensity (I_{lim}) for each feed pressures applied to the cell and for a range of salinity prepared with sodium chloride solution. The results allow the potential relationship between the limiting current densities (i_{lim}) and the product flow (Q_p) to be established and extrapolated to a complete pilot plant EDR.

Keywords: Ion-exchange membranes; Electro dialysis reversal; Optimization; Desalination; Polarization; Hydrodynamic regime

1. Introduction

Ion-exchange membranes are used in electro dialysis (ED) to desalinate aqueous electrolytic solutions through a process of ion-selective migration, when a potential difference between two electrodes at either side of the membrane system is applied. The direction and velocity of ion transport depends on the charge

and mobility of each ion, the conductivity of the ionic solution, the relative concentrations of the ions, the potential difference applied, etc. (Fig. 1(a)) [1,2]. The performance of the process is limited by the effects of concentration–polarization at the membrane–solutions interfaces, in where the current initially grows linearly with the electric voltage applied, before moderating its growth to reach a “plateau” characterized by the limiting current intensity (I_{lim}) (Fig. 1(b)) [3].

*Corresponding author.

Presented at the IX Ibero-American Congress on Membrane Science and Technology (CITEM 2014), 25–28 May 2014, Santander, Spain

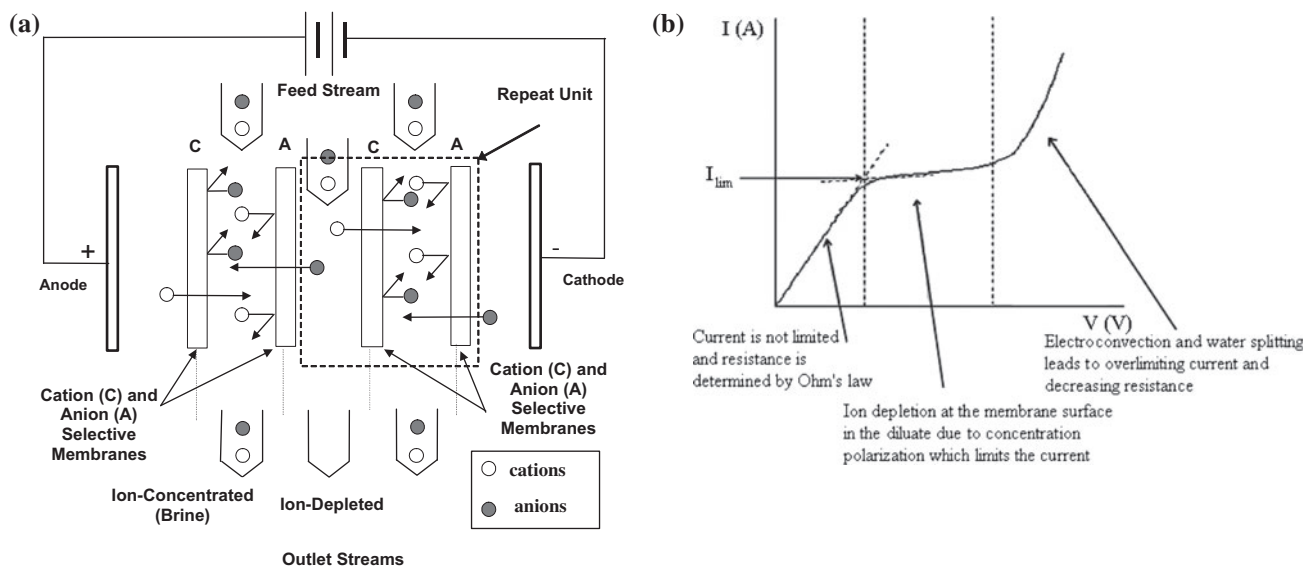


Fig. 1. (a) Principle of ED. Scheme of an electrodyalizer with two cell pairs: the migration of ions is caused by the action of an electric field; (b) Outline of a current–voltage curve corresponding to an ED cell operated at constant solution flow velocities.

The correct current–voltage characterization of an electro dialysis reversal (EDR) plant is important and of great interest for determining the limiting current intensities for the complete membrane system (membrane + diffusion boundary layer), as easily and accurately as possible. Previously, [4,5] we studied certain aspects related to EDR pilot plants, with determining the most favourable experimental conditions for desalination by using scanning voltage at different pressures. The aim of this work is to ascertain the limiting current densities (i_{lim}) for an ED cell of an EDR pilot plant, at different feed pressures (and therefore feed flow, Q_a) by drawing tangents in the “plateau” zone and the first ascending section of the I – V curves. The results provide a characterization of the hydrodynamic regime of the system, in the flow and salinity ranges considered.

2. Theory

2.1. Limiting current density

This phenomenon has been studied widely [6–10] and is responsible for decreasing the concentration of electrolyte on the side of the membrane in contact with the diluate compartment, while increasing the concentration on the other side in contact with the concentrate compartment. The phenomenon is due to the existence of a difference between the ionic mobility of the counterions at the membrane and solutions in contact with it.

According to the classical theory of concentration–polarization for ion-exchange membranes [11], the current–voltage shows three sections in the steady-state response [6]. For the first section, at low current intensities, there is a linear dependence between the current and the applied voltage [12]; in the second section, the current varies very slowly with the applied voltage reaching the “plateau” zone, which corresponds to the so-called limiting current; in the third section, the current intensity increases with the applied voltage again.

Basically, the system under consideration consists of an exchange membrane separating two electrolyte solutions (1:1) whose concentrations in the bulk solutions are C_0 and C_0' , respectively, under the same pressure and temperature conditions (Fig. 2). When an electrical potential difference is applied, the electric current through the membrane system increases the motion of coions and counterions in the boundary diffusion layers at both sides of the membrane, while inside the membrane the current is mainly transported by the counterions. The current lowers the concentration inside the electrolyte diffusion layers in contact with the dilute compartment (C_1), while increasing the concentration in the diffusion layers in contact with the concentrate compartment (C_2). Both concentrations C_1 and C_2 are related with concentrations at the membrane interfaces (Fig. 2) in the case of current densities, such as $i < i_{lim}$, the concentrations C_1 and C_2 at the membrane solution interfaces are given as a function of bulk concentrations C_0 and C_0' by [5]:

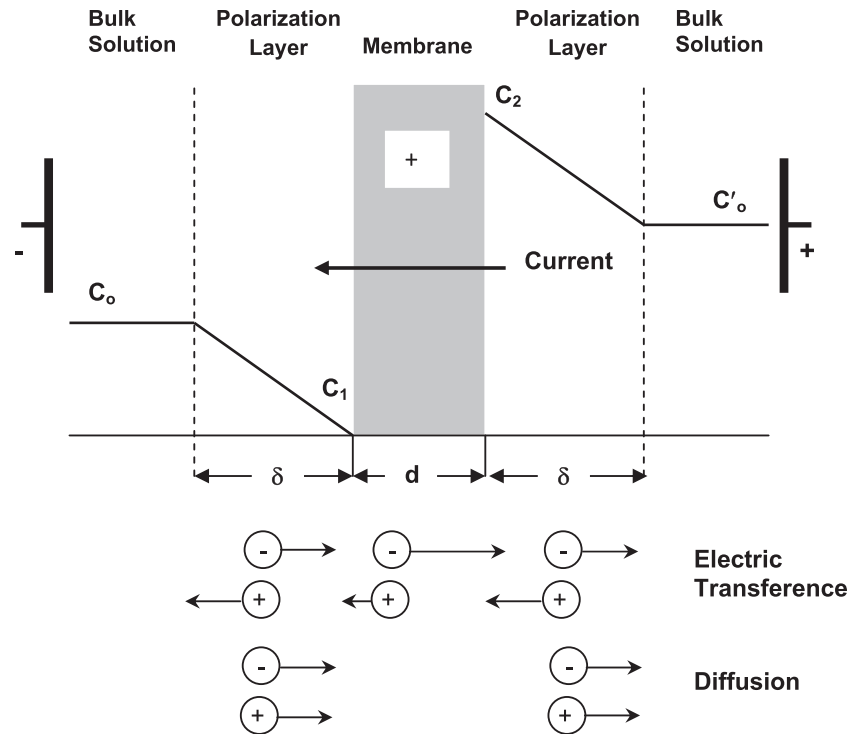


Fig. 2. Counterion concentration profile in the polarization layers in an ion-exchange membrane. d and δ are the thickness of the membrane and layers, respectively. The arrows show the transport rate of different ions.

$$C_1 = C_0 \left(1 - \frac{i}{i_{\text{lim}}} \right); C_2 = C_0' \left(1 + \frac{i}{i_{\text{lim}}} \right) \quad (1)$$

In this way, the I - V curves show a less pronounced slope. When this effect continues indefinitely, a “plateau” is reached because the depletion layer resistance tends to infinity, while the interfacial concentration falls to zero.

In this situation, a concentration gradient through the boundary layers of both sides of the membrane is established. In these polarization layers, the electric potential gradient leads anions and cations in opposite directions, while the concentration gradient leads both ion types in the same direction (diffusion). The limiting current corresponds to the minimum electrolyte concentration in one side of the membrane/solution interface. When the current exceeds the limiting current, the effect of concentration polarization increases due to the combination of a number of effects, such as the dissociation of water, the exaltation of ionic fluxes [13–15] and gravitational convection (for a certain range of salt concentrations). The gravitational effect of convection and exaltation contribute to the increased mass transfer. The exaltation of the ionic

fluxes is due to the electric field created by the H^+ and OH^- ions produced in the dissociation of water. This phenomenon causes a change in the pH in the channels of the concentrate and diluate solutions, the pH increasing at the surface of the anion exchange membrane and decreasing at the surface of the cation exchange membrane, which may lead to the precipitation of carbonates and calcium and magnesium sulphates. This is why it is important to determine the limiting current intensity.

Depending on the design of an ED cell, and its practical operating conditions providing product concentration in relation with flow and concentration feed, it is necessary to minimize the polarization effects, either by reducing the current density or by diminishing the thickness of the boundary diffusion layer. This thickness is determined by the hydrodynamic conditions of fluid circulation, which depends on spacers and the speed of circulation in the hydraulic channels.

Theoretically, it is possible to obtain the limiting current density for the condition of zero concentration at the interface between the membrane surface and boundary diffusion layer whose ionic concentration has decreased, obtaining the following expression [11,12,16,17]:

$$i_{\text{lim}} = \frac{D_s FC_0}{\Delta t_j \delta} \quad (2)$$

where δ denotes the boundary layers thickness and $\Delta t_j = \bar{t}_j - t_j$ the difference between the counterion transport number in the membrane and free solution, with $t_j = J_j F / i$ and $\bar{t}_j = \bar{J}_j F / i$ (univalent ions), i being the current density and J_j (\bar{J}_j) the flux associated to ions in the bulk solution and membrane, respectively. D_s is the electrolyte diffusion coefficient.

Generally, the thickness of the diffusion boundary layer of an ED cell is difficult to measure experimentally, although it is related with the diffusion coefficient of the electrolyte through the mass transfer coefficient k , defined as [18]:

$$k = \frac{D_s}{\delta} \quad (3)$$

which is a function of the hydrodynamic conditions of the ED cell, i.e. the fluid velocities in the channels of the solution, the design geometry of the cell and spacer and the diffusion coefficient of the salt. So Eq. (2) gives:

$$i_{\text{lim}} = \frac{FC_0}{\Delta t_j} k \quad (4)$$

The limiting current density of an ED cell relates to the average linear velocity of the solution flow in the desalination channels parallel to the membrane surface through equation [19–24]:

$$i_{\text{lim}} = \alpha C v^\beta \quad (5)$$

where C is the electrolyte concentrations in the inlets of the desalination channels and α and β are constants to be determined experimentally. The parameter α only depends on the desalination channel geometry and membrane nature, while β depends on the hydrodynamic regime: $\beta=0.33$ is the laminar regime; $\beta=0.4-0.5$ is the transition regime and $\beta=0.7-1.0$ corresponds the turbulent regime [25,26].

2.2. Hydrodynamic

The hydrodynamic design of an ED system has special relevance for calculating the cost of the product because it is necessary to control the operating current density and power consumption used to mix and circulate the solution through the system. Both

aspects are related to mass transfer and the friction characteristics of the ED system.

Any ED hydrodynamic design of a system employing turbulence promoters requires knowledge of its geometry and of the velocity of the fluid circulating through the channels.

For a given design, mass transfer can be related to the Sherwood number (Sh) [27–31], expressed as a function of the limiting current density and friction factor (λ) [27,28], which is related to the pressure drop (ΔP) in the channel through which fluid flows. Regardless of size, the hydrodynamic performance of a system is completely defined when these two dimensionless parameters are related to the Reynolds number (Re) [27,31].

For the ED system, we consider a model of a hydraulic channel of length L (Fig. 3(a)), a cross flow of ionic solution with a velocity v and a mean current density i over the membrane area A , as a consequence of an applied potential difference, V , across thickness h (distance between membranes, i.e. channel width of the product). The fluid stream is due to a pressure difference, ΔP , along the length L . For a suitable working hydrodynamic system, the operating current density (i_{op}) should not exceed the limiting current density and the pressure difference should not be excessive.

The limiting current density can be expressed as a function of the Sherwood number according to expression [27]:

$$\text{Sh} = i_{\text{lim}} h / D_s FC \quad (6)$$

where F is the Faraday constant, D_s is the diffusion coefficient of the salt (which for simplicity, will be assumed valid for both anions and cations) and C is the average value of the ionic concentration at the inlet and outlet of the product channel. For a system with a given geometry, the Sherwood number depends only on the number Re and the Schmidt number (Sc), whose expressions are [27–31]:

$$\text{Re} = v \rho h / \mu \text{ and } \text{Sc} = \mu / \rho D_s \quad (7)$$

ρ and μ being the fluid density and viscosity coefficient, respectively.

When the channels have turbulence promoters, the Sherwood number will depend on the geometric arrangement of the same (parameter $\Delta L/h$, where ΔL is the distance between the two strips of mesh spacers of thickness h). When $\Delta L \ll h$ and the solution concentration does not vary much along the hydrodynamic channel, the mass transfer is fully controlled by turbulence promoters. In this case, a relation between the

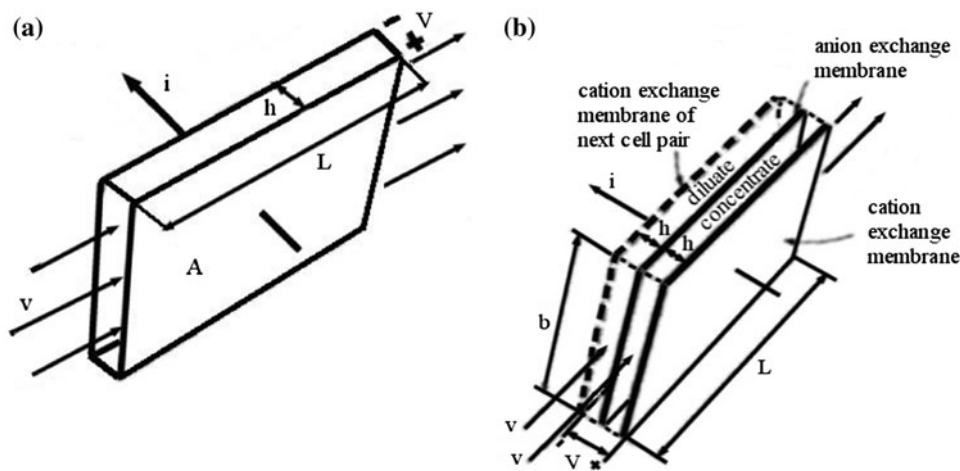


Fig. 3. (a) Flow channel in ED half cell. i is the current density; (b) Flow channel in complete ED cell.

Sherwood number and Reynolds number is obtained, describing mass transport by convective–diffusion (neglecting free convection), given by [32,33]:

$$\text{Sh} = B(\text{Sc})^\gamma \text{Re}^\beta \quad (8)$$

where B , γ and β are empirical constants. B is a constant, whose value depends on the diffusion coefficient, viscosity and density near the membrane [32]. For a relatively thin channel, the value of exponent γ is typically taken to be $1/3$, based on hydrodynamic theory, and so Eq. (8) reduces to:

$$\text{Sh} = B(\text{Sc})^{1/3} \text{Re}^\beta \quad (9)$$

In this manner, a plot of the Sherwood number vs. the Reynolds number will provide the parameters B and β .

The pressure difference (ΔP) can be expressed as a function of the dimensionless parameter λ named friction factor and given by Darcy, whose expression is [28,34]:

$$\lambda = \frac{\Delta P}{\frac{L}{h} \cdot \frac{1}{2} \rho v^2} \quad (10)$$

If the flow is totally viscous and the channels are free (with no turbulence promoters), the pressure difference is given by [35]:

$$\Delta P = \frac{32vL\mu}{h^2} \quad (11)$$

Substituting the last equation in Eq. (10) gives:

$$\lambda = 64 / \text{Re} \quad (12)$$

When the turbulence promoters in the channels have a given particular geometry, we can define a modified friction factor, f , as a function of friction factor λ , and the Reynolds number takes the form:

$$f = (\lambda)^{1/3} \text{Re} = (64)^{1/3} \text{Re}^{2/3} \quad (13)$$

In this way, both magnitudes the Sherwood number and the friction factor (dependent on the Reynolds number), can be related through a functional dependence of $\text{Sh} = m f^n$ type, where m and n are dimensionless parameters related to the characteristics of the optimal operation of the hydrodynamic system [27,28].

Let us consider an ED cell (Fig. 3(b)) and assume that the two channels, diluate and concentrate, have the same width h and length L , the same solution velocity v , and feed solution concentration C_a and product solution concentration C_p , respectively, corresponding to the inlet and outlet of the diluted channel. For each Faraday of current passing perpendicularly through the channel, an equivalent of salt from the solution of the channel is transported from the dilute to concentrate, and if we assume there is no concentration polarization, the average current density can be expressed by [27]:

$$i = \frac{\sigma \Delta V}{h} \quad (14)$$

where σ is the mean conductivity of the solution between the electrodes and ΔV is the potential

Table 1
Specifications of the ED cell

Type	Filter press	Ionic [®] Aquamite I
ED Cell	Number	1
	Ion-exchange membranes	1 cell pair
	Size of membranes	23.0 × 25.5 cm ²
	Spacer MK I	Thickness (h): 1 mm Flow path length: 348 cm
Operating conditions	Effective area per membrane	230 cm ²
	Flow rate of water in cell	13–50 l/h
	Current density (A/m ²)	2.04–3.30
	Pressure range	0.15–0.45 atm
	Voltage range	0.5–5.0 V
Standard feed water	Salt	Sodium chloride
	Concentration	Low salinity: 1,060 mg/l
	Temperature	Inlet: 20°C Outlet: 20–25°C

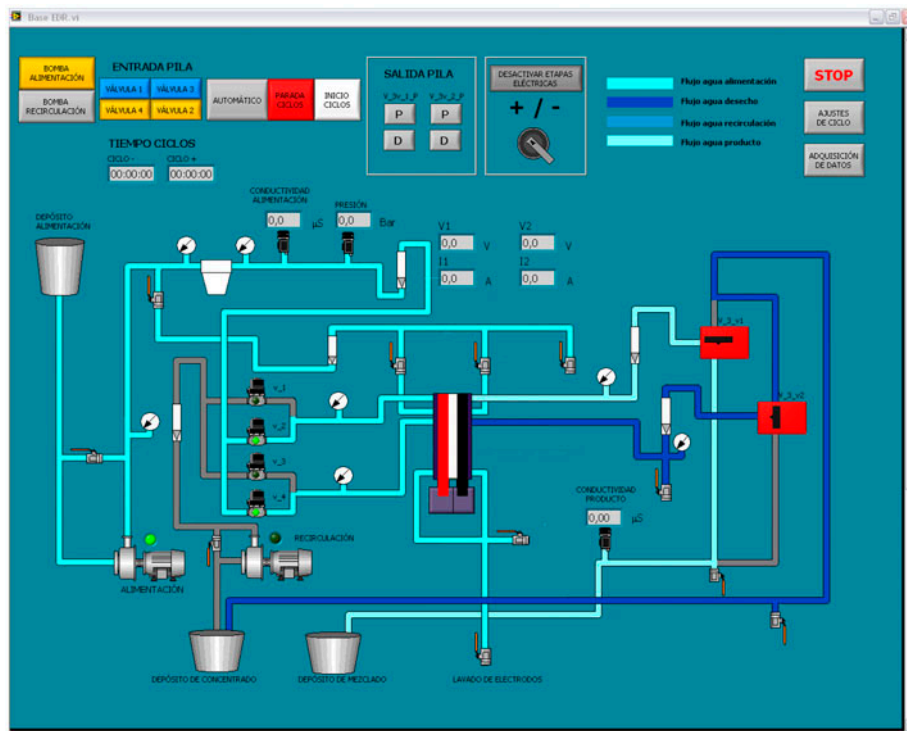


Fig. 4. Application SCADA for our ED cell.

difference established between them. Also, if the conductivity is given in all cases by [27]:

$$\sigma = \frac{2ZF^2D_sC}{RT} \quad (15)$$

with $C = [(C_a + C_p)/2]$ and T being the absolute temperature and R the universal perfect gas constant. Substituting Eq. (14) into Eq. (15) we can obtain the correlation between the current density and the mean concentration of the solution in the diluted channel.

Table 2

Results characterizing our ED cell (see list of symbols) at different pressures considered with effective membrane area of $(230 \pm 2) \text{ cm}^2$ with $C_p = 1,060 \text{ ppm}$. The errors of different magnitudes ε are indicated

$(P \pm 0.01) \text{ (atm)}$	0.15	0.20	0.25	0.30	0.35	0.40	0.45
$(Q_p \pm 0.1) \times 10^6 \text{ (m}^3/\text{s)}$	3.6	5.5	7.2	8.9	10.5	12.2	13.9
$v \text{ (m/s)}$	0.55	0.84	1.09	1.30	1.60	1.80	2.10
$\varepsilon [v] \text{ (m/s)}$	0.07	0.11	0.13	0.20	0.21	0.22	0.24
$(t \pm 0.01) \text{ (s)}$	6.37	4.14	3.18	2.59	2.18	1.88	1.66
$(V \pm 0.01) \text{ (V)}$	1.90	2.16	2.37	2.57	2.80	3.00	3.16
$i_{lim} \text{ (A/m}^2)$	2.04	2.26	2.48	2.69	2.91	3.13	3.30
$\varepsilon [i_{lim}] \text{ (A/m}^2)$	0.06	0.06	0.06	0.07	0.07	0.07	0.07
Sh	240	290	320	350	380	400	420
$\varepsilon [\text{Sh}]$	30	30	40	40	50	50	50
Re	546	840	1,090	1,340	1,600	1850	2,100
$\varepsilon [\text{Re}]$	13	20	20	30	30	40	50
λ	0.12	0.08	0.06	0.05	0.04	0.03	0.03
$\varepsilon [\lambda]$	0.03	0.02	0.01	0.01	0.01	0.01	0.01
f	270	360	420	490	550	600	660
$\varepsilon [f]$	8	11	11	14	14	17	21
$((i_{lim}/C_p) \pm 1) \text{ ((A m)/eq)}$	35	42	47	51	55	58	60
$\ln v$	-0.60	-0.17	0.09	0.26	0.47	0.59	0.74
$\varepsilon [\ln v]$	0.08	0.02	0.01	0.04	0.06	0.07	0.08
$\ln ((i_{lim}/C_p) \pm 0.01)$	3.56	3.74	3.85	3.93	4.00	4.05	4.10
$k \times 10^4 \text{ (m/s)}$	3.6	4.4	5.0	5.2	5.7	6.00	6.30
$\varepsilon [k] \text{ (m/s)}$	0.8	1.0	1.1	1.2	1.3	1.3	1.4
η	0.43	0.55	0.64	0.73	0.81	0.89	0.96
%S	99.68	99.70	99.71	99.71	99.71	99.70	99.69

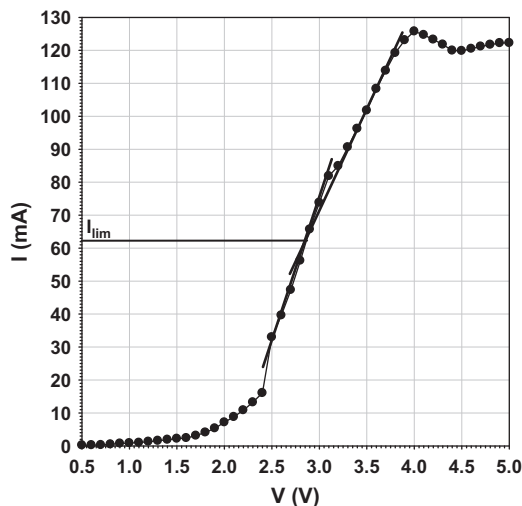


Fig. 5. Current intensity vs. applied voltage at 0.3 atm. The straight tangent lines corresponding to the two central sections, whose intersection gives the limiting current, are drawn. The standard solution employed in our study was a sodium chloride aqueous solution with a conductivity of $1,635 \mu\text{S/cm}$ (1,060 ppm).

3. Experimental

In this paper, we have obtained the limiting current density in a electrolysytic cell (anion membrane

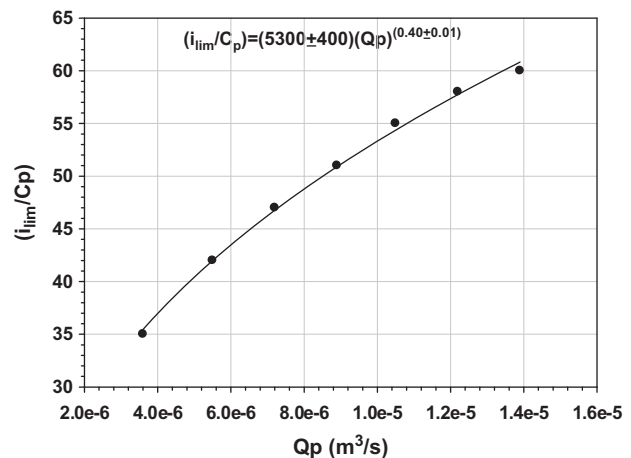


Fig. 6. Limiting current density as a function of product flow. The curve was determined by fitting a power function of two parameters with a correlation coefficient of 0.999.

AR204SZRA and cation membrane CR64LMR, both 0.5 mm thick) belonging to a reversible stack (EDR) Aquamite I of Ionics, with MKI tortuous path spacers (1 mm thick) where the solution flows along a narrow channel with nine 180° turns between the inlet and outlet of the compartment [36]. The spacers determine

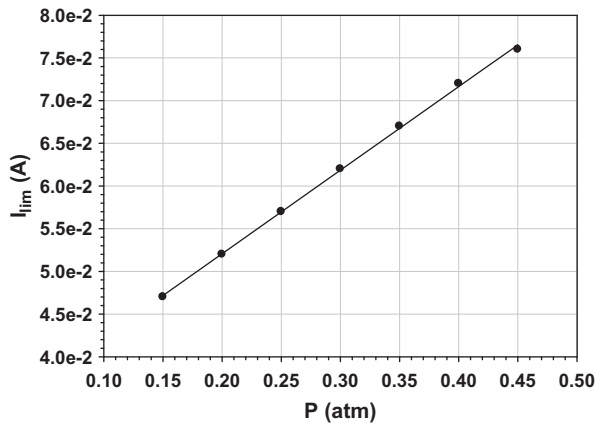


Fig. 7. Limiting current intensity vs. feed pressure with fitting a straight line by least-square analysis.

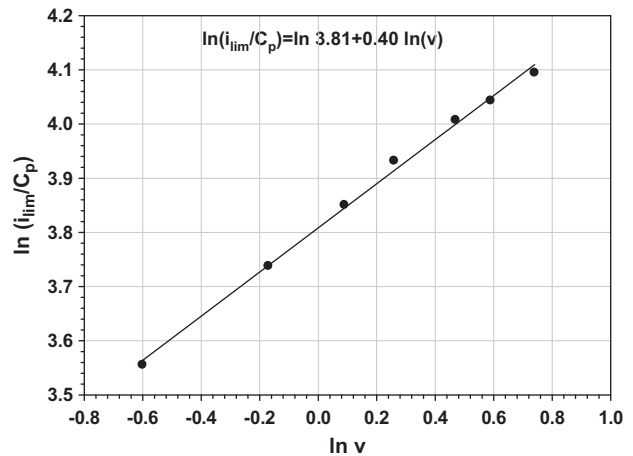


Fig. 9. Natural logarithm of (i_{lim}/C_p) vs. natural logarithm of v in the cell. The straight line corresponds to the suitable fitting by least-square analysis.

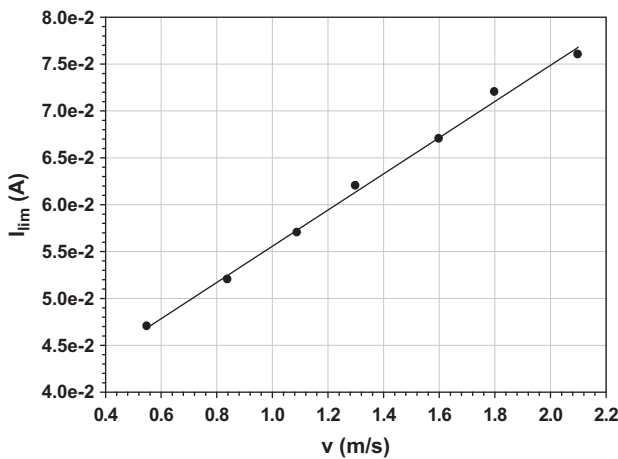


Fig. 8. Limiting current intensity vs. mean velocity in the flow channels (see Table 2). A straight line adjust by least-square analysis are shown.

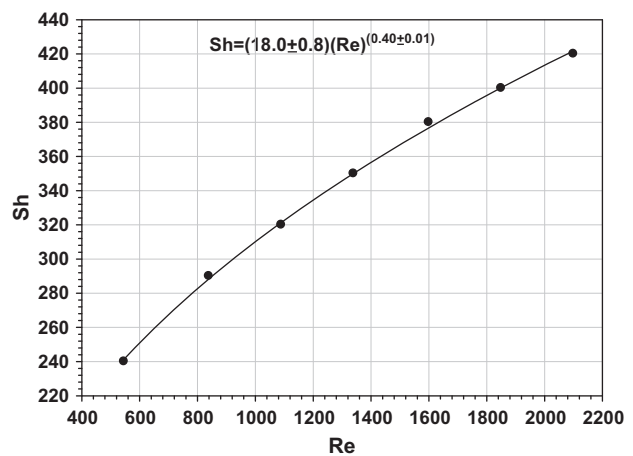


Fig. 10. Sherwood number against Reynolds number in the cell. The curve was determined by fitting a power function of two parameters with a correlation coefficient of 0.999.

an effective transfer area in the membrane of 230 cm^2 and channel length of 348 cm. The set is placed between two platinized titanium electrodes, with an effective area of 550 cm^2 , and are continually rinsed with feed water with a flow of 101/h. The characterization was carried out by applying the same pressure input channels (P) to the ED cell and, for every value, electric voltage (V) scans of between 0.5 and 5.0 V in steps of 0.1 V. The gauge pressure varies between 0.15 and 0.45 atm, and the mean value of the current in the cell is determined for each voltage and applied pressure (Table 1).

The ED cell was characterized by desalting a standard aqueous solution, prepared with degassed

deionised water and sodium chloride, with a conductivity of $1,635 \mu\text{S}/\text{cm}$ (1,060 ppm low concentration brackish water type) and a pH of 6.0. The salt used was of analytical grade. Typical values of an aqueous salt solution ($D_s = 1.5 \times 10^{-9} \text{ m}^2/\text{s}$; $\rho = 10^3 \text{ kg}/\text{m}^3$; $\mu = 10^{-3} \text{ kg}/\text{m s}$) were taken for the fluid [27].

The process control and data acquisition is fully automated using an Omron PLC, model CPM1 20CDR-A, and a National Instruments model NI USB-6210 data acquisition card. A SCADA application was designed with the LabVIEW development version 9.0. The PLC is charged with operating the plant, controlling the feed pump, recirculation pump, inlet valves to the stack, three-way battery output valves, applied

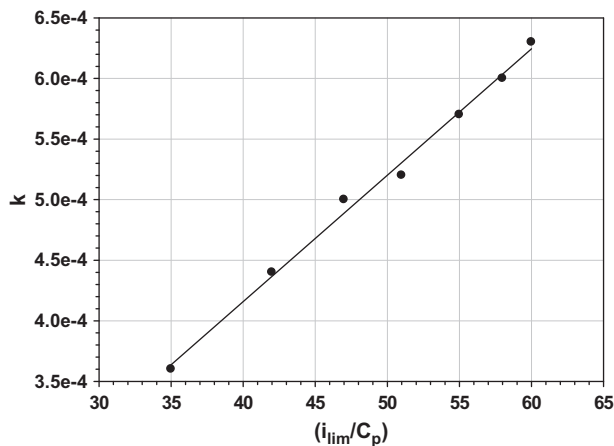


Fig. 11. Mass transfer coefficient k vs. (i_{lim}/C_p) in the cell.

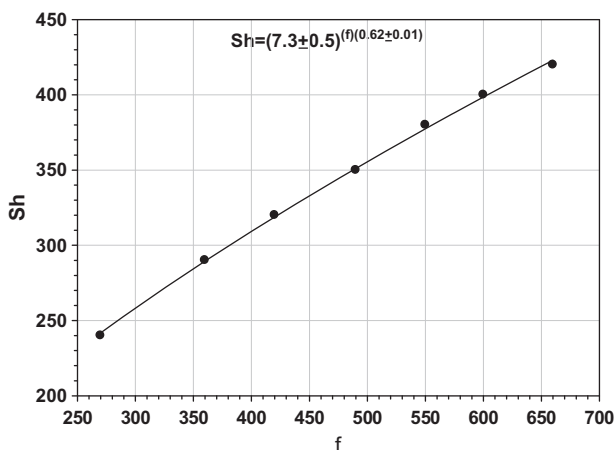


Fig. 12. Sherwood number against modified friction factor in the cell. The curve was determined by fitting a power function of two parameters with a correlation coefficient of 0.999.

electrical potential difference and changes in polarity when working with recirculation cycles. With the data acquisition card, the analogical data is converted into a digital signal and sent to the SCADA application. The data treated were inlet pressure, voltage and currents of the electrical stage, and the conductivities of feed water, product water and wastewater. The SCADA application provides a graphical interface (Fig. 4) to control the PLC, allowing communication with the card, reading and storage of the data collected.

For each pressure and applied voltage, three measurements were taken and average values are reported.

4. Results and discussion

The current intensity in the ED cell for each applied voltage and pressure drop was recorded, as

were the values of the feed flow, product flow and waste flow rates with their respective conductivities. In this way, the values of the I_{lim} and i_{lim} for each feed pressure were obtained (Table 2). As we can see in Fig. 5, and given that commercial ED systems typically operate at high Re numbers in contrast to laboratory systems operating at low Re numbers, the “plateau” does not appear; instead, a dramatic change in the I – V curve slope is evident [28].

I – V curves were drawn for each pressure (Fig. 5) and as product concentrations under the same conditions were obtained. From these curves, limiting current densities (i_{lim}) were determined, and according to their dependence on the flow rate product (Q_p), relations $(i_{lim}/C_p) = aQ_p^\beta$ were obtained, with $\beta \approx (0.40 \pm 0.01)$ (s/m³) and $a(5,200 \pm 400)$ ((A m)/eq). The results were similar to that described by Eq. (5) (Fig. 7). On the other hand $(i_{lim}/C_p) = \alpha v^\beta$ follows with $\beta \approx (0.40 \pm 0.01)$ (s/m) and $\alpha(45.15 \pm 0.13)$ ((A m)/eq) for the considered salinity.

With the velocity values obtained, the Reynolds number was calculated, and the limiting current density provided the Sherwood number (Table 2). In this way, the potential relationship that appears in Eq. (8) was obtained (Fig. 10).

The limiting current intensity for each applied pressure was determined from the intersection of tangents corresponding to the portions of the curve at the point where slope changes. Fig. 8 illustrates the values of I_{lim} as a function of the feed pressure. Table 2 also shows i_{lim} vs. mean velocity in dilute channel, whose values are represented in Fig. 9. The mean velocity agreed with the manufacturer’s data [36] (see Table 1).

The electric current density in an electrochemical cell is related to the average fluid velocity in the channels (v) by Eq. (3). Thus, (Fig. 6) $\ln(i_{lim}/C) - \ln(v)$ shows a linear behaviour, which can be extrapolated to each one of the electrical stages of an EDR pilot plant.

Substituting i_{lim} of Eq. (4) in Eq. (6) gives the Sherwood number as a function of the mass transfer coefficient and the current density limit (Fig. 11). In addition, a functional dependence between the Sherwood number and the modified friction factor f was obtained (Fig. 12).

Table 2 illustrates all the values of the experimental results obtained in this paper.

5. Conclusions

- (1) An ED cell was characterized by obtaining the current–voltage curves for each of the pressures considered.

- (2) From these curves, the limiting current intensity was determined, and subsequently, the current limiting densities, which increased linearly with respect to the applied pressure.
- (3) The limiting current densities were correlated with the values of velocity and product flow rate, allowing potential type relationships to be established in both cases.
- (4) The Sherwood and Reynolds numbers were correlated over the laminar regime range, showing a potential dependence with an identical exponent that corresponds to the limiting current referred to in point (3). In the same way, the Sherwood number correlated with the modified friction factor in the ED cell, which also shows a potential dependence.
- (5) With respect to the experimental device, the automated system allows data control and management in real-time, enabling immediate reconfiguration if necessary.

List of symbols

A	— longitudinal section area of the hydraulic channel (m^2)	t_i	— counterion transport number in free solutions
B	— dimensionless constant	\bar{t}_i	— counterion transport number in the membrane
C_0, C_0'	— bulk electrolyte concentrations (eq/m^3)	T	— absolute temperature (K)
C_1, C_2	— electrolyte concentrations (eq/m^3) on the membrane (depletion and concentration layers, respectively)	v	— flow velocity (m/s)
C_a	— feed concentration (eq/m^3)	V	— applied electric voltage (V)
C_p	— product concentration (eq/m^3)	Z	— ion charge number
d	— thickness of the membrane (m)	δ	— boundary layers thickness (m)
D_s	— electrolyte diffusion coefficient (m^2/s)	λ	— friction factor
F	— Faraday constant, 96,490 (C/eq)	μ	— solution viscosity ($\text{kg}/\text{m s}$)
f	— modified friction factor	ρ	— solution density (kg/m^3)
h	— width of the hydraulic channel (m)	σ	— electrical conductivity (S/m)
i_{lim}	— limiting current density (A/m^2)		
I_{lim}	— limiting current intensity in the ED cell (A)		
k	— coefficient of mass transfer (m/s)		
L	— flow path length in each spacer (m)		
ΔL	— separation between successive eddy promoters (m)		
ΔP	— pressure drop in the flow direction (N/m^2)		
P	— feed solution pressure (atm)		
Q_a	— feed flow (m^3/s)		
Q_p	— product flow (m^3/s)		
R	— universal gas constant, 8.31 (J/K mol)		
Re	— Reynolds number		
Sc	— Schmidt number		
Sh	— Sherwood number		
Δt_j	— difference between the counterion transport numbers in the membrane and free solutions		

References

- [1] J.J. Krol, M. Wessling, H. Strathmann, Concentration polarization with monopolar ion exchange membranes: current–voltage curves and water dissociation, *J. Membr. Sci.* 162 (1999) 145–154.
- [2] P.M. Bungay, H.K. Lonsdale, M.N. de Pinho, *Synthetic Membranes: Science, Engineering and Applications*, D. Riedel Pub. Co., Dordrecht, 1986.
- [3] P. Długolecki, B. Anet, S.J. Metz, K. Nijmeijer, M. Wessling, Transport limitations in ion exchange membranes at low salt concentrations, *J. Membr. Sci.* 346 (2010) 163–171.
- [4] R. Valerdi-Pérez, M. López-Rodríguez, J.A. Ibáñez-Mengual, Characterizing an electro dialysis reversal pilot plant, *Desalination* 137 (2001) 199–206.
- [5] R. Valerdi-Pérez, J.A. Ibáñez-Mengual, Current–voltage curves for an electro dialysis reversal pilot plant: Determination of limiting currents, *Desalination* 141 (2001) 23–37.
- [6] I. Rubinstein, L. Shtilman, Voltage against current curves of cation exchange membranes, *J. Chem. Soc., Faraday Trans.* 75 (1979) 231–246.
- [7] V. Aguilera, S. Mafe, J.A. Manzaneres, J. Pellicer, Current–voltage curves for ion-exchange membranes. Contributions to the total potential drop, *J. Membr. Sci.* 61 (1991) 177–190.
- [8] Y. Tanaka, Concentration polarization in ion exchange membrane electro dialysis, *J. Membr. Sci.* 57 (1991) 217–235.
- [9] V.M. Barragan, C. Ruiz-Bauzá, Current–voltage curves for ion-exchange membranes: A method for determining the limiting current density, *J. Colloid Interface Sci.* 205 (1998) 365–373.
- [10] H. Strathmann, Electro dialysis, a mature technology with a multitude of new applications, *Desalination* 264 (2010) 268–288.
- [11] F. Helfferich, *Ion-exchange*, Mc Graw-Hill, New York, NY, 1962.
- [12] H. Strathmann, *Synthetic membranes in science, engineering and applications*, in: P.M. Bungay, H.K. Lonsdale, M.N. de Pinho (Eds.), *Proc. NATO Adv. Inst.*, Lisboa, 1983, Kluwer, Dordrecht, 1986, p. 197.
- [13] I. Rubinstein, B. Zaltzman, O. Kedem, Electric fields in and around ion-exchange membranes1, *J. Membr. Sci.* 125 (1997) 17–21.

- [14] V.I. Zabolotsky, V.V. Nikonenko, N.D. Pismenskaya, E.V. Laktionov, M.Kh. Urtenov, H. Strathmann, M. Wessling, G.H. Koops, Coupled transport phenomena in overlimiting current electro dialysis, *Sep. Purif. Technol.* 14 (1998) 255–267.
- [15] E.V. Laktionov, N.D. Pismenskaya, V.V. Nikonenko, V.I. Zabolotsky, Method of electro dialysis stack testing with the concentration regulation, *Desalination* 151 (2002) 101–116.
- [16] M. Taky, G. Pourcelly, F. Lebon, C. Gavach, Polarization phenomena at the interfaces between an electrolyte solution and an ion exchange membrane, *J. Electroanal. Chem.* 336 (1992) 171–194.
- [17] Y. Tanaka, Mass transport in a boundary layer and in an ion exchange membrane: Mechanism of concentration polarization and water dissociation, *Russ. J. Electrochem.* 48 (7) (2012) 665–681.
- [18] V. Geraldes, M.D. Afonso, Limiting current density in the electro dialysis of multi-ionic solutions, *J. Membr. Sci.* 360 (2010) 499–508.
- [19] Y. Tanaka, Current density distribution and limiting current density in ion exchange membrane electro dialysis, *J. Membr. Sci.* 173 (2000) 179–190.
- [20] Y. Tanaka, Current density distribution, limiting current density and saturation current density in an ion-exchange membrane electro dialyzer, *J. Membr. Sci.* 210 (2002) 65–75.
- [21] L. Hong-Joo, F. Sarfert, H. Strathmann, M. Seung-Hyeon, Designing of an electro dialysis desalination plant, *Desalination* 142 (2002) 267–286.
- [22] Y. Tanaka, Limiting current density of an ion-exchange membrane and of an electro dialyzer, *J. Membr. Sci.* 266 (2005) 6–17.
- [23] L. Hong-Joo, H. Strathmann, M. Seung-Hyeon, Determination of the limiting current density in electro dialysis desalination as an empirical function of linear velocity, *Desalination* 190 (2006) 43–50.
- [24] V. Silva, E. Poiesz, P. van der Heijden, Industrial wastewater desalination using electro dialysis: Evaluation and plant design, *J. Appl. Electrochem.* 43 (2013) 1057–1067.
- [25] D.M. Malone, J.L. Anderson, Diffusional boundary-layer resistance for membranes with low porosity, *AIChE J.* 23 (1977) 177.
- [26] S. Hwang, K. Kammermeyer, *Membranes in Separation*, Wiley, New York, NY, 1975.
- [27] A.A. Sonin, M.S. Isaacson, Optimization of flow design in forced flow electrochemical systems, with special application to electro dialysis, *Ind. Eng. Chem. Process Des. Dev.* 13(3) (1974) 241–248.
- [28] A.A. Sonin, M.S. Isaacson, Sherwood number and friction factor correlations for electro dialysis systems, with application to process optimization, *Ind. Eng. Chem. Process Des. Dev.* 15(2) (1976) 313–321.
- [29] M. Sadrzadeh, A. Kaviani, T. Mohammadi, Mathematical modeling of desalination by electro dialysis, *Desalination* 206 (2007) 538–546.
- [30] H. Xu, W. Huang, Y. Xing, H. Lin, H. Ji, M. Jiang, X. Liu, S. Gan, Effect of configuration on mass transfer in a filter-press type electrochemical cell, *Chin. J. Chem. Eng.* 16(2) (2008) 198–202.
- [31] V.V. Nikonenko, N.D. Pismenskaya, A.G. Istoshin, V.I. Zabolotskii, A.A. Shudrenko, Generalization and prognostication of mass exchange characteristics of electro dialyzers operating in overlimiting current regimes with use made of similarity theory and compartmentation method, *Russ. J. Electrochem.* 43(9) (2007) 1069–1081.
- [32] A.A. Kozinski, E.N. Lightfoot, Protein ultrafiltration: A general example of boundary layer filtration, *AIChE J.* 18 (1972) 1030–1040.
- [33] V.I. Zabolotskii, V.V. Nikonenko, Electro dialysis of dilute electrolyte-solutions—Some theoretical and applied aspects, *Russ. J. Electrochem.* 32 (1996) 223–230.
- [34] H. Schlichting, *Boundary-layer Theory*, McGraw-Hill, New York, NY, 1979.
- [35] P. Tsiakis, L.G. Papageorgiou, Optimal design of an electro dialysis brackish water desalination plant, *Desalination* 173 (2005) 173–186.
- [36] F.H. Meller, *Electro dialysis & electro dialysis reversal technology*, in: F.H. Meller (Ed.), Ionics Incorporated, Watertown, MA, 1984, pp. 23–47.